Chemistry–A European Journal
Research Article
doi.org/10.1002/chem.202201480
Chemistry Europe
European Chemical Societies Publishing
www.chemeurj.org

Reversible Oxidative Addition of Zinc Hydride at a Gallium(I)-Centre: Labile Mono- and Bis(hydridogallyl)zinc Complexes

Louis J. Morris,[a, b] Thayalan Rajeshkumar,[c] Laurent Maron,*[c] and Jun Okuda*[a]

Abstract: In the presence of TMEDA (*N,N,N′,N′*-tetramethylethylenediamine), partially deaggregated zinc dihydride as hydrocarbon suspensions react with the gallium(I) compound [(BDI)Ga] (**I**, BDI = {HC(C(CH$_3$)N(2,6-*i*Pr$_2$-C$_6$H$_3$))$_2$}$^-$) by formal oxidative addition of a Zn–H bond to the gallium(I) centre. Dissociation of the labile TMEDA ligand in the resulting complex [(BDI)Ga(H)–(H)Zn(tmeda)] (**1**) facilitates insertion of a second equiv. of **I** into the remaining Zn–H to form a thermally sensitive trinuclear species [{(BDI)Ga(H)}$_2$Zn] (**2**). Compound **1** exchanges with polymeric zinc dideuteride [ZnD$_2$]$_n$ in the presence of TMEDA, and with compounds **I** and **2** via sequential and reversible ligand dissociation and gallium(I) insertion. Spectroscopic and computational studies demonstrate the reversibility of oxidative addition of each Zn–H bond to the gallium(I) centres.

Introduction

The diverse and versatile reactivity of main-group (MG) metal hydrides has resulted in their widespread application as stoichiometric and catalytic reagents in organic and inorganic synthesis.[1] Meanwhile, transition metal (TM) hydrides are key intermediates in vital catalytic processes such as (de)hydrogenation,[2] hydroformylation,[2b,3] Fischer–Tropsch synthesis,[4] and the Haber-Bosch process.[5] Recent years have seen a revived interest in molecular (hetero)bimetallic complexes which display potentially advantageous synergistic effects.[6] Reaction of a MG hydride with a low-coordinate TM complex can provide a multinuclear complex in which the metal centres are bound by one or more bridging hydrides, by a metal-metal bond derived from formal oxidative addition, or a bonding situation between these extremes (Scheme 1, **A**).[7] Such species can participate as reactive intermediates in challenging catalytic transformations including C–H metalation of arenes,[8] C–O activation,[9] and hydrodefluorination.[10] Following analogies between the frontier molecular orbital situation of transition metals and low-valent main group complexes,[11] heterobimetallics based exclusively on MG elements may have the potential to exhibit similarly useful reactivity. In this vein, Harder and et al. demonstrated the calcium-catalysed alumination of benzene, which likely involves a highly reactive heterobimetallic Al–Ca intermediate formed by formal oxidative addition of a Ca–H bond to the Al(I) centre.[12] Structurally characterised magnesium and zinc analogues [(BDI)Al(H)–M{BDI}] (BDI = {HC(C(CH$_3$)N(2,6-*i*Pr$_2$-C$_6$H$_3$))$_2$}$^-$; M = Mg, Zn) were prepared by this method, but proved inert towards benzene.[12] More generally, the formation of dinuclear main group complexes via formal oxidative addition of a MG–X bond to a low valent MG centre has been well documented,[13] but reversibility has only been demonstrated in a few cases[13c–f,14] and subsequent reactivity studies remain scarce (Scheme 1, **A**). We recently reported the oxidative addition of [(tmeda)AlH$_2$(OEt$_2$)][BAr$_4^{Me}$] (TMEDA = *N,N,N′,N′*-tetramethylethylenediamine, BAr$_4^{Me}$ = [B(3,5-Me$_2$-C$_6$H$_3$)$_4$]$^-$) to the gallium(I) compound [(BDI)Ga] (**I**; Scheme 1, **B**).[15] Formation of a non-dative Ga–Al bond in the product [(BDI)Ga(H)–(H)Al-Al(tmeda)][BAr$_4^{Me}$] (**II**) may be rationalised by relief of electron deficiency at the cationic aluminium centre provided by generation of a strongly σ-donating hydridogallyl ligand.[16] Reductive elimination of [L$_n$AlH$_2$]$^+$ remains energetically viable and occurs spontaneously when electron deficiency is instead relieved by THF or N-heterocyclic carbenes (NHCs).[15]

Although the TM-mediated chemistry of diorganozinc reagents ZnR$_2$ has been investigated in detail,[17] analogous low-valent MG-mediated organozinc reactivity remains underexplored.[14f,18] Examples of zinc-containing heterometallic hydride complexes are numerous,[7f,h,k,m,n,8b,17g,j,19] but we are unaware of any that derive directly from the parent dihydride

[a] Dr. L. J. Morris, Prof. Dr. J. Okuda
Institute for Inorganic Chemistry
RWTH Aachen University
52062 Aachen (Germany)
E-mail: jun.okuda@ac.rwth-aachen.de
Homepage: http://www.okuda.ac.rwth-aachen.de/
[b] Dr. L. J. Morris
Chemistry Research Laboratory
University of Oxford
Oxford OX1 3TA (United Kingdom)
[c] Dr. T. Rajeshkumar, Prof. Dr. L. Maron
CNRS, INSA, UPS, UMR 5215, LPCNO
Université de Toulouse
31077 Toulouse (France)
E-mail: laurent.maron@irsamc.ups-tlse.fr

Supporting information for this article is available on the WWW under https://doi.org/10.1002/chem.202201480

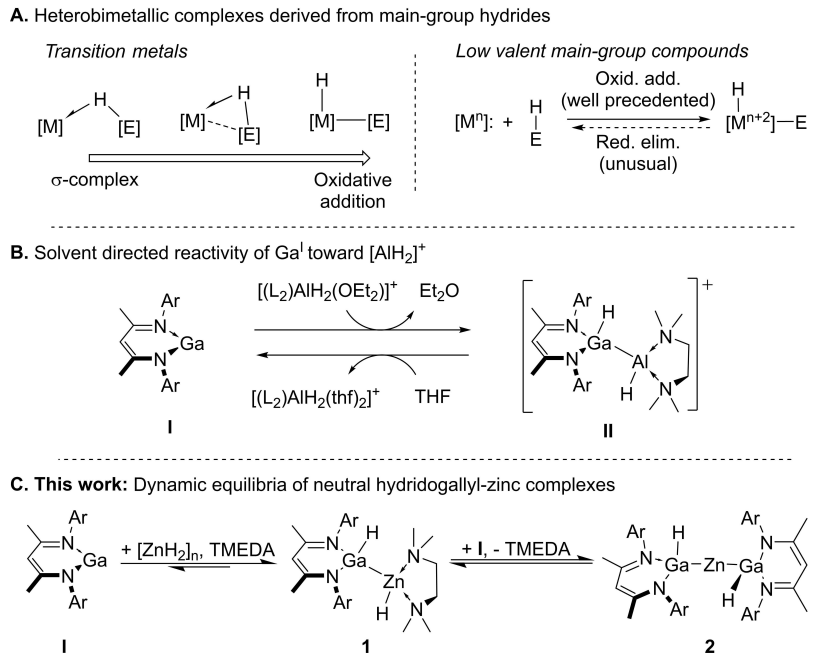

Scheme 1. Generalised reactivity patterns of main-group hydrides with transition metals (**A**, left) and low-valent main-group compounds (**A**, right); Solvent directed selectivity of oxidative addition and reductive elimination of cationic aluminium hydrides to gallium(I) compound **I** (**B**);[15] TMEDA-mediated equilibria of compound **I** with neutral zinc dihydride (**C**, this work). TMEDA = *N,N,N′,N′*-tetramethylethylenediamine; Ar = 2,6-*i*Pr$_2$-C$_6$H$_3$.

$[ZnH_2]_n$. This lacuna is unsurprising given that polymeric $[ZnH_2]_n$ is insoluble in organic solvents, thermally sensitive, and challenging to synthesise in an analytically pure form.[20] The presumed polymeric structure of $[ZnH_2]_n$ can be disrupted by N-heterocyclic carbenes (NHCs) or by chelating *N*-donors, which activate the monomeric units towards Lewis acids and electrophiles, thus resulting in soluble molecular species.[21] Noting that main-group centred oxidative addition and reductive elimination may also be controlled by (de)coordination of neutral donors,[15,22] we resolved to probe the chemistry of TMEDA-deaggregated $[ZnH_2]_n$ within the coordination sphere of **I** (Scheme 1, **C**). The results of this study are disclosed herein.

Results and Discussion

NHCs were previously shown to completely deaggregate $[ZnH_2]_n$, providing soluble and thermally robust dimers $[(NHC)Zn(H)(\mu\text{-}H)]_2$.[21c] Following the isolobal analogy between NHCs and group 13 carbenoids,[23] $[ZnH_2]_n$ was suspended in a C_6D_6 solution of compound **I**.[24] Analysis of the reaction mixture by ^{1}H NMR revealed a lack of reactivity and only slight decomposition of $[ZnH_2]_n$ was observed over the course of 3 days. Heating the reaction mixture to 70 °C for 3 h, however, resulted in a 1:4 mixture of **I** and $[(BDI)GaH_2]$ (**I-H$_2$**)[25] with concomitant formation of a dark grey precipitate, presumably metallic zinc (Scheme 2). Although **I** has been reported to react with 1 bar H_2 to form **I-H$_2$** at room temperature,[26] C_6D_6 solutions of **I** are inert under H_2 atmosphere (ca. 1.5 bar) up to at least 70 °C in our hands. Indeed, Power et al. showed that related terphenyl-gallium(I) complexes react with H_2 only in

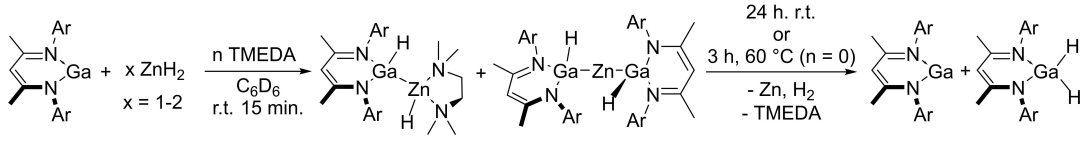

n =	1	2	I	I-H$_2$
0	0	0	18%	82%
0.1	5%	90% (16%)	50%	50%
1.2	65%	19%	27%	73%
5	>99% (56%)	0	0	0

Scheme 2. Reaction of compound **I** with $[ZnH_2]_n$ in the presence of TMEDA to provide **1** and/or **2**. Yields determined were by ^{1}H NMR spectroscopy. Isolated yields after workup on preparative scale are shown in parentheses. Ar=C$_6$H$_3$-2,6-*i*Pr$_2$.

their dimeric "digallene" form;[27] similar dimerization is less feasible for the more sterically demanding BDI-system.[24] We have found that **I** is able to react with H_2 in the presence of Lewis-acidic zinc hydride cations, whilst the direct oxidative addition of H_2 to the Ga(I) centre of **I** was calculated to be kinetically unfeasible and only weakly exothermic.[28] It is plausible that the originally reported oxidative addition was promoted by Lewis acidic impurities. Generation of **I-H$_2$** during the thermal decomposition of $[ZnH_2]_n$ in the presence of **I** thus implies direct zinc-to-gallium hydride transfer via thermally unstable multinuclear heterometallic intermediates, as opposed to reaction of **I** with H_2 derived from the decomposition of zinc dihydride into its elements.

The reaction was repeated in the presence of 1.2 equiv. of TMEDA, and a homogeneous bright yellow solution was obtained after two minutes. Analysis of this sample by ^{1}H NMR spectroscopy showed 75% conversion of **I** to two new BDI-containing products, [(BDI)Ga(H)–(H)Zn(tmeda)] (**1**) and [{(BDI)-Ga(H)}$_2$Zn] (**2**), in an approximate 3:1 ratio (Scheme 2). Immediate workup and recrystallisation from an *n*-hexane/toluene mixture at −35 °C provided single crystals of compound **1** as yellow blocks in 47% yield. If the reaction mixture was instead left to stand for 24 h, both species were consumed with concomitant (re)formation of **I**, **I-H$_2$**, and metallic zinc. Repeating the reaction under a five-fold excess of TMEDA provided compound **1** as the sole product, crystallised on a larger scale in 56% yield. Selective formation of compound **2** was observed when a catalytic quantity of TMEDA (0.1 equiv.) was employed, and yellow rod-like single crystals suitable for X-ray diffraction analysis were obtained after recrystalising the crude product from a concentrated *n*-pentane solution at −35 °C. Owing to low thermal stability and redistribution in solution (see below), however, reproducibly isolating bulk quantities of compound **2** proved problematic.

The solid-state structures of compounds **1** and **2** were elucidated by single-crystal X-ray diffraction. Compound **1** crystallises from *n*-hexane/toluene as yellow blocks in the orthorhombic space group *Pnma*, with half a molecule per asymmetric unit such that C3, Ga1, H1, Zn1 and H2 are bisected by a mirror plane (Figure 1a). The ethylene backbone of the TMEDA ligand was disordered across the mirror plane in two components of equal occupancy. The two metal centres each adopt a distorted tetrahedral geometry and are joined by a Ga–Zn bond 2.4348(16) Å in length. A terminal hydride ligand bound to each metal centre was located and freely refined, such that the dinuclear H1-Ga1-Zn1-H2 unit adopts an antiperiplanar conformation. In addition to heterometallic clusters,[29] several prior examples of unsupported Ga–Zn bonds have been

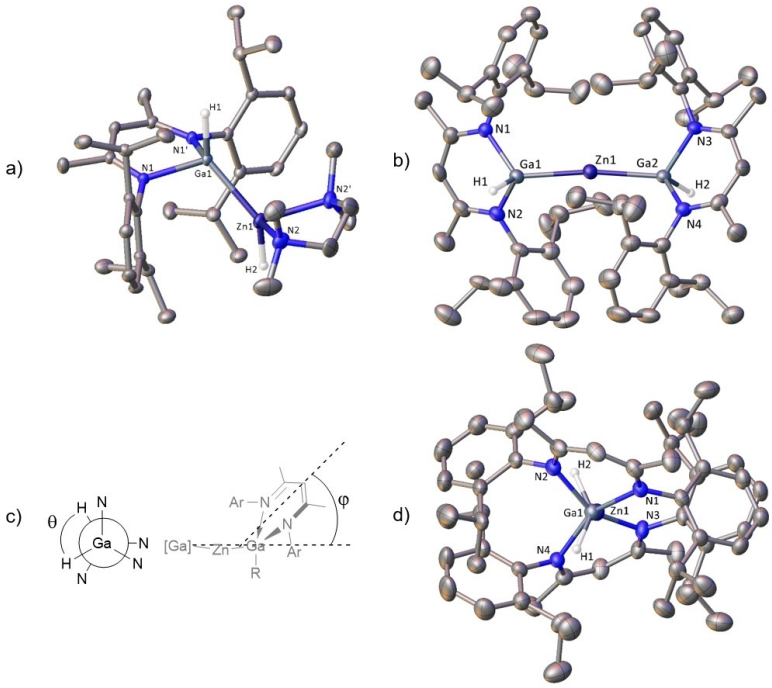

Figure 1. X-ray crystal structure of a) **1** and b) **2**; c) representation of HGaGaH dihedral torsion angle θ and fold angle φ between the Ga–Ga axis and NCCCN plane of the BDI ligand in compounds **2** and **III**;[18a] d) view down the Ga1-Ga2 axis of **2**. Except for metal-bound hydrides, hydrogen atoms are omitted for clarity. Only one of the two crystallographically independent molecules of compound **2**, and only the major component of disordered *isopropyl* groups are shown. Only one component of the TMEDA-backbone disorder in compound **1** is shown. Displacement parameters are shown at the 50% level. Selected distances (Å) and angles (°) for **1**: Ga1-Zn1 2.4348(6), Ga1-N1/N1′ 2.0353(15), Zn1-N2/N2′ 2.2237(18), Ga1-H1 1.55(3), Zn–H2 1.51(3), N1/N1′-Ga1-Zn1 113.38(4), N1′-Ga1-N1 90.63(8), N2/N2′-Zn1-Ga1 113.89(5), N2-Zn1-N2′ 82.58(10), H1-Ga1-Zn1 133.9(10), Ga1-Zn1-H2 136.5(13). Symmetry operations to generate primed atoms: +x, 3/2–y, +z. Selected distances (Å) and angles (°) for Zn1-centred molecule of **2**: Ga1-Zn1 2.4334(12), Zn1-Ga2 2.4338(12), Ga1-N2 1.994(4), Ga1-N1 1.993(4), Ga2-N4 1.994(4), Ga2-N3 1.992(4), Ga1-H1 1.51(4), Ga2-H2 1.63(4), N2-Ga1-Zn1 111.79(13), N1-Ga1-Zn1 118.08(12), N1-Ga1-N2 92.41(17), Ga1-Zn1-Ga2 172.68(2), N4-Ga2-Zn1 111.47(13), N3-Ga2-Zn1 118.03(13), N3-Ga2-N4 93.14(17). For a table including selected distances and angles for the Zn2-centred molecule of **2**, see Supporting Information.

crystallographically characterised,[18,29c,30] albeit hydride-substituted complexes of this type have not been previously reported. The metal-metal bond of **1** is significantly elongated compared to those of other non-dative dinuclear Ga–Zn compounds (2.3230-2.4107(5) Å).[18a–c,28,30b,c] The Ga–N bonds of **1** (2.0353(15) Å) are of intermediate length relative to **I** (2.0528(14), 2.0560(13) Å)[24a] and **I-H$_2$** (1.960(1), 1.963(1) Å),[25] consistent with partial oxidation of the gallium(I) centre. Crystallographically characterised [(tmeda)ZnXX′] moieties cover a wide range of Zn–N distances, and the Zn1–N2 distance of **1** (2.2237(18) Å) is unremarkable in this respect. Compound **1** is structurally similar to dihydridogallyl-aluminylium cation **II**.[15] Aside from slightly longer Ga–N bond lengths, which likely reflect the more electron rich bimetallic core of the neutral molecule, the H1-Ga1-Zn1 (133.9(10)°) and Ga1-Zn1-H2 (136.5(13)°) angles are both significantly wider than the analogous angles in **II** (H1-Ga1-Al1, 117.1(9)°; Ga1-Al1-H2, 126.7(9)°).

The crystal structure of compound **2** (Figure 1b) was solved in the non-centrosymmetric orthorhombic space group, *Pca2$_1$*, with two crystallographically independent molecules per asymmetric unit. Aside minor differences that presumably arise from packing forces, the two molecules are similar, with a near-linear (172.58(2)°, 173.35(2)°) trinuclear Ga–Zn–Ga core. An unsupported Ga–Zn-Ga unit was previously reported in Fischer's closely related methyl complex [{(BDI) GaMe}$_2$Zn] (**III**),[18a] and Jones's [({^{Dipp}DAB}Ga)$_2$Zn(tmeda)] (^{Dipp}DAB = [(2,6-*i*Pr$_2$-C$_6$H$_3$)NC(H)=C(H)N((2,6-*i*Pr$_2$-C$_6$H$_3$))]$^{2-}$).[18c] The two-coordinate zinc centre of **2** is located centrally (within experimental error) between two hydridogallyl units of distorted tetrahedral geometry, akin to the trimetallic core of **III**. Direct bonding interaction between the hydrides and central zinc atom are ruled out by the long distances between these atoms (H1-Zn1, H2-Zn1; 3.48(4) Å, 3.62(4) Å). The Ga–Zn distances of **2** (Ga1–Zn1, Zn1–Ga2; 2.4334(12), 2.4338(12) Å, respectively) are similar to that of compound **1** (2.4348(6) Å), but slightly shorter than those of **III** (2.4631(7), 2.4609(7) Å).[18a] Like **III**, the {(BDI)GaX} units adopt a staggered conformation when viewed down the Ga–Ga axis, yet the H1-Ga1-Ga2-H2 dihedral angle is much larger (θ = 134.4(19)°, vs. C2-Ga1-Ga2-C41 θ = 93.41(17)° for **III**). This conformational discrepancy is also reflected in the N–Ga-Ga–N torsion angles (see Supporting Information, Table S4). Presumably due to additional steric pressure imposed by the methyl substituents, the NCCCN planes of **III** are near-perpendicular to the Ga–Ga axis (fold angle (Figure 1c) $\phi \approx$ 74, 90°), minimising steric clash between the staggered Dipp substituents. By contrast, the analogous angles of **2** are much smaller ($\phi \approx$ 25°) and the Dipp groups face towards the centre of the molecule, such that two of the four aromatic substituents are near-eclipsed (Figure 1d). The importance of attractive intramolecular dispersion forces between sterically demanding ligand substituents has been previously highlighted,[31] and similar forces may be in effect here.

The solid-state (KBr) IR spectrum of **1** contains two absorptions at ν = 1641 and 1581 cm^{-1}, which are respectively assigned to the Ga–H and Zn–H stretching modes. The Ga–H stretching absorption of **2** was assigned to a sharp band at ν = 1638 cm^{-1}. The significant redshift relative to **I-H$_2$** (ν = 1893 and 1861 cm^{-1})[25] and molecular zinc hydrides,[21b,c] is consistent with the relatively electron-rich bimetallic core.

Compounds **1** and **2** were analysed computationally at the DFT level (B3PW91). Gas-phase optimised structures were in good agreement to the crystallographically determined structures. NBO analysis shows the HOMO of compound **1** (Figure 2) to be represented by the Ga–Zn bond with significant delocalisation over both hydride ligands, whilst the LUMO is based on the BDI ligand. This contrasts with the situation in **II**, where the M–H σ-bonding electrons occupied lower lying molecular orbitals and the LUMO involved an Al–Ga π-orbital.[15] The Wiberg Bond Index (WBI) of the Ga–Zn bond is 0.85, consistent with a covalent single bond. The bond is polarised Ga$^{\delta+}$–Zn$^{\delta-}$ (natural charges 0.71 (Ga), 0.55 (Zn)), and 64% of the electron density is contributed by the gallium centre. As expected, both metal-hydride bonds are polar-covalent in nature, with WBI values of 0.77 (Ga–H) and 0.64 (Zn–H) and 70%/76% contribution from the respective hydrides. The HOMO of compound **2** (Figure 2) is delocalised over the entire H–Ga-Zn-Ga–H unit, whilst the LUMO is ligand-based. The Ga–Zn bonds are derived from overlap of *s* (45%) *p* (55%) orbitals of the terminal gallyl ligands (70% gallium contribution) with similarly hybridised orbitals of the central zinc atom (*s* 50%; *p* 50%). The delocalised bonding situation is reflected in the WBI values of 0.64 (Ga–Zn) and 0.20 (Ga–Ga), and each metal carries a comparable charge (0.58, Ga; 0.62, Zn). The bonding situation is reminiscent to that of the central [Zn$_3$]$^{2+}$ unit in Jones's comparable linear trizinc complex [(L*Zn)$_2$Zn] (**IV**, L* = N(2,6-{C(H)Ph$_2$}$_2$-4-Me-C$_6$H$_2$)(Si*i*Pr$_3$)). The central zinc atom of **IV** was formally assigned the oxidation state zero, with a natural charge of only 0.18 (vs. 0.62 for **2**). The two-coordinate terminal zinc atoms of **IV** were calculated to engage in metal-metal bonding exclusively through the valence s-orbitals.[32] A BDI-supported trizinc complex was also reported by Crimmin and et al.[10b] Based on the relative Pauling electronegativity values of gallium (1.81) and zinc (1.65),[33] the metals in compound **2** are assigned the respective formal oxidation

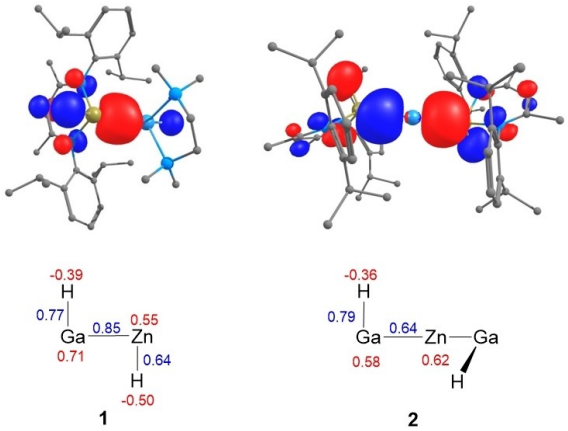

Figure 2. DFT calculated HOMO (top), Wiberg Bond Indices (WBIs, bottom, blue), and Natural Charges (bottom, red) of compounds **1** (left), and **2** (right).

states of +1 and +2. The high covalency and delocalisation of electron density across the trinuclear core suggested by computational data, however, suggests that suggests non-negligible contributions by the resonance forms [(BDI)(H)Ga^{I}→Zn^{I}–Ga^{II}(H)(BDI)] in addition to that implied on the basis of electronegativity and formal oxidation state alone [(BDI)(H)Ga^{I}→Zn^{II}←Ga^{I}(H)(BDI)].

Benzene solutions of compound **1** are stable at ambient temperature in the presence of excess (>5 equiv.) TMEDA for at least one week. The ^{1}H NMR spectrum of a TMEDA-stabilised C_6D_6 solution is consistent with retention of the solid-state structure in solution. The C_s-symmetry of compound **1** is reflected in the appearance of two septets and four doublets pertaining to the *isopropyl* protons of the Dipp substituents. The γ-methine signal of the BDI-backbone appears at δ_H = 4.86 ppm whilst the respective gallium and zinc-bound hydrides resonate as a pair of mutually coupled doublets at δ_H = 6.32, 4.52 ppm ($^{3}J_{HH}$ = 12.3 Hz). The hydride resonances fall within the typical chemical shift range of gallium and zinc hydrides. Although of a similar magnitude to that observed in **II** ($^{3}J_{HH}$ = 11.0 Hz),[15] the coupling constant is much larger than typical for $^{3}J_{HH}$ coupling through a metal-metal bond ($^{3}J_{HH}$ ≈ 3–6 Hz),[34] a feature that is indicative of restricted rotation about a highly covalent bond. Correct assignment is supported by ^{1}H-^{1}H NOESY experiments, which showed intramolecular through-space coupling between the metal hydrides and nearby *N*-methyl and/or *isopropyl* protons of the supporting ligands. Two broad resonances were assigned to free TMEDA in rapid intermolecular exchange with a second, even broader TMEDA environment in the δ_H = 1.5–2.0 ppm range. The exchange process was indicated by cross peaks of positive phase in the corresponding ^{1}H-^{1}H NOESY spectrum. Assignment of the latter signal to zinc-ligated TMEDA was supported by recording a ^{1}H NMR spectrum of isolated crystals of **1** in C_6D_6, without additional equivalents of stabilising TMEDA. Aside from minor variations in chemical shift and apparent coupling constant, this NMR spectrum is otherwise identical to that recorded in the presence of excess TMEDA. Tellingly, however, a minor quantity of free TMEDA was also observed in this solution, along with 0.1 equiv. of **2**. These observations provide evidence for both facile dissociation of TMEDA, and reductive elimination of ZnH_2 from **1** with respective generation of unsaturated intermediate [(BDI)(H)Ga–ZnH] (**1′**) and **I**. Recombination of these species generates trimetallic **2** by oxidative addition of the Zn–H bond. Over the course of 16 h, C_6D_6 solutions of pure **1** partially decompose with precipitation of metallic zinc to yield TMEDA, **I** and **I-H$_2$**. Decomposition was completed by heating the mixture to 60 °C for one hour, providing **I** and **I-H$_2$** as the only soluble BDI-containing species in a 1:3 ratio. A signal at δ_H = 4.47 ppm was assigned to H_2 derived from thermal decomposition of ZnH_2 into its elements.

Further evidence for reductive elimination of ZnH_2 from **1** was gleaned whilst studying the reaction between **I** and a slight excess of $[ZnH_2]_n$ (1.2 equiv.) in the presence of 5 equiv. of TMEDA by in situ ^{1}H NMR spectroscopy. It was noticed that both hydride signals of the product **1** appeared as broadened singlets instead of the well-resolved doublets observed for isolated samples. After 20 h. at room temperature, decomposition of the excess $[ZnH_2]_n$ to its elements was evident by formation of a grey precipitate, and the hydride doublets of **1** were resolved. It was hypothesised that these observations derive from rapid exchange between compound **1** and solvated oligomeric clusters "$[(ZnH_2)_x(tmeda)_y]$", which decompose over time. Limited spectroscopic evidence for such species was provided by analysing suspensions of $[ZnH_2]_n$ in a C_6D_6 solution of 5 equiv. of TMEDA by ^{1}H NMR spectroscopy; a broad signal observed at δ_H = 4.57 ppm was tentatively ascribed to soluble zinc hydride species. Further, **1/1-d$_2$** slowly exchanges with excess $[ZnD_2]_n$/$[ZnH_2]_n$ in the presence of 5 equiv. of TMEDA, respectively (see Supporting Information for details).

The ^{1}H NMR spectrum of freshly dissolved crystals of **2** is consistent with the solid-state structure, and agrees with the in situ NMR spectrum of the reaction between **I** and $[ZnH_2]_n$ in the presence of 0.1 equiv. of TMEDA. The γ-methine proton resonates at δ_H = 4.68 ppm and the gallium-hydrides appear as a broad singlet δ_H = 5.86 ppm. Two overlapping septets at δ_H = 3.25–3.46 ppm belonging to the BDI-isopropyl groups indicate a greater degree of conformational flexibility compared to the relatively congested bimetallic core of compound **1**. Additional resonances, however, already hint at the low thermal stability of this compound and within 10 h at 25 °C, quantitative disproportionation to an equimolar solution of **I** and **I-H$_2$** was observed with concomitant precipitation of metallic zinc (Scheme 2). Analogies can be drawn to Harder's trimagnesium complex [(^{tBu}BDI^{Dipep})Mg–Mg–Mg(^{tBu}BDI^{Dipep})] (^{tBu}BDI^{Dipep} = HC{C(*t*Bu)N(2,6-(C(H)Et$_2$)$_2$-C$_6$H$_3$)}$_2$), which eliminates metallic magnesium at 80 °C with formation of a Mg(I) dimer, [{κ$_1$-^{tBu}BDI^{Dipep}}Mg–Mg{κ$_2$-^{tBu}BDI^{Dipep}}].[35] Jones's linear trizinc complex **IV** was also reported to slowly decompose in both solution and solid state with deposition of metallic zinc, although the other products were not identified.[32] It is plausible that decomposition of **2** proceeds via an undetected dinuclear intermediate [(BDI)(H)Ga–Ga(H)(BDI)], which rapidly disproportionates to the observed products. Consistent with this proposal, the aluminium congener [(BDI)(H)Al–Al(H)(BDI)] is known to disproportionate to [(BDI)AlH$_2$] and [(BDI)Al] in C_6D_6 solution at 50 °C.[13c]

The labile nature of both complexes prompted a more detailed analysis of the dynamic solution-state behaviour. Addition of a C_6D_6 solution of compound **2** to a seven-fold excess of TMEDA resulted in immediate formation of **1** and **I** in equimolar ratio (Scheme 3a).[36] Furthermore, dissolving an equimolar mixture of **I** and **1** in toluene-d_8 provided a 2:2:1:1 mixture of **I**, **1**, **2**, and TMEDA (Scheme 3b). Acquisition of a ^{1}H-^{1}H NOESY spectrum at 0 °C with a 400 ms evolution time showed, in addition to expected intramolecular NOE and through-bond coupling correlations, intermolecular correlation peaks of positive phase, indicative of chemical exchange on the timescale of the experiment (Figure 3). Specifically, the gallium-hydride resonance of **2** at δ_H = 5.77 ppm exchanges with both the gallium- and zinc hydride resonances of **1** (δ_H = 6.23, 4.44 ppm, respectively). Similarly, evidence for exchange between **1** and **2**, and between **2** and **I**, but not between **I** and **1** (on the 400 ms timescale) was provided by cross-peaks

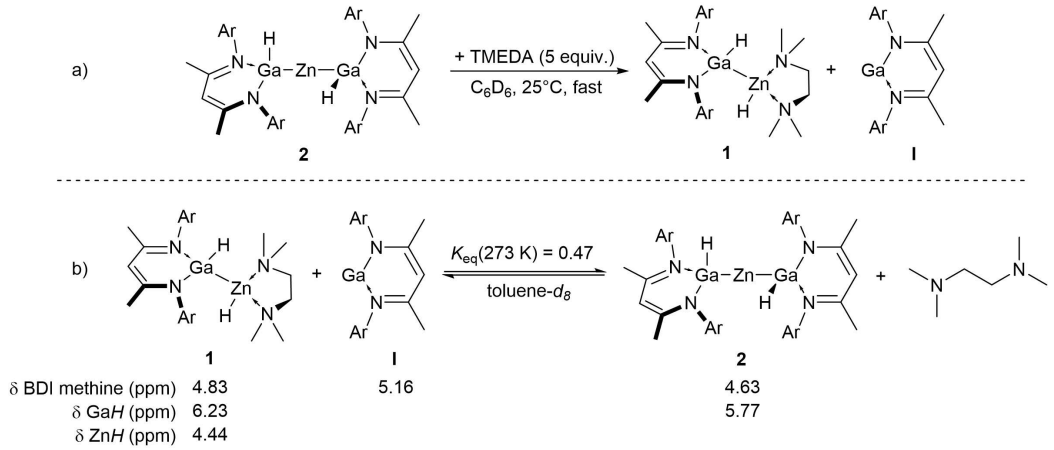

Scheme 3. Stoichiometric experiments demonstrating the TMEDA-controlled interconversion of **1** and **2** via oxidative addition and reductive elimination of Zn–H bonds. Chemical shifts of key resonances in the ^{1}H NMR shown for (b). Ar=C_6H_3-2,6-*i*Pr_2.

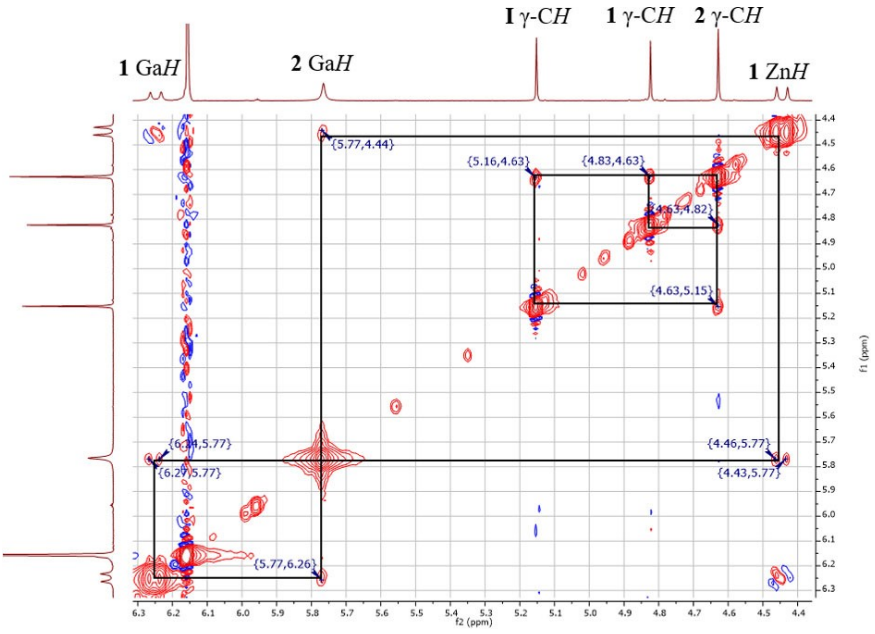

Figure 3. Expanded NOESY spectrum (400 MHz, toluene-d_8, 273 K, 400 ms evolution time) obtained from the equimolar reaction of **I** and **1** (Scheme 4b), highlighting cross-peaks indicative of exchange between **I** and **2**, and between **2** and **1**.

correlating to the γ-methine signals of the respective BDI ligand backbones (Figure 3). Similar intermolecular exchange peaks were observed between resonances of TMEDA in its complexed and un-complexed forms (see Supporting Information). When the mixing time was decreased to 250 ms, only a weak signal for **I**–**2** exchange was detected, and no cross peaks were observed for exchange between **1** and **2**, but pronounced correlation between coordinated and free TMEDA remained. This indicates that the kinetics of ligand dissociation are faster compared to oxidative addition and reductive elimination of Zn–H bonds, and supports the hypothesis that formation of **2** from **1** occurs in a stepwise fashion via **I**. These observations account for the TMEDA-dependent selectivity observed in the synthesis of **1** and **2**, and confirm the reversible, *N*-donor controlled nature of oxidative addition and reductive elimination of Zn–H bonds in this system. The thermodynamics of this equilibrium (Scheme 3b) were quantified by van't Hoff analysis over the temperature range 247–278 K, returning values of $\Delta H = 22.0\ kJ\,mol^{-1}$, $\Delta S = 73.5\ JK^{-1}\,mol^{-1}$. Below 247 K, substantial signal broadening likely indicative of slower kinetics prevented acquisition of meaningful van't Hoff plots, especially considering the near thermoneutrality of this equilibrium (ΔG-(298 K) = 0.1 $kJmol^{-1}$). These observations are complementary to recent work by the Aldridge group, who showed that reductive elimination and oxidative addition of tin hydrides to a formally Sn(I) centre was controlled by (de)coordination of a hemilabile ligand.[22c]

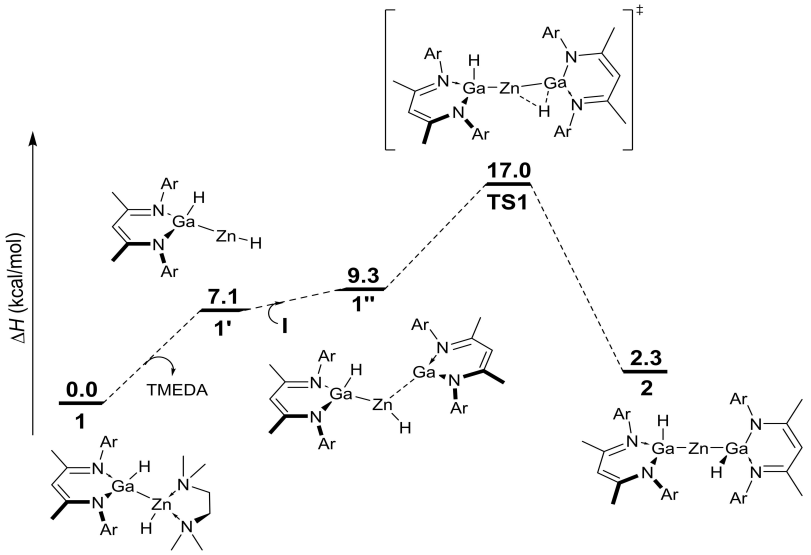

Figure 4. DFT calculated reaction pathway for the reaction between **1** and **I**. See Supporting Information for full details; Ar=C_6H_3-2,6-*i*Pr_2.

The interconversion of **1** and **2** was investigated computationally using Density Functional Theory (DFT) at the B3PW91 level including solvent (benzene, see Supporting Information for details). Consistent with experimental observations, the overall process was calculated to be almost thermoneutral, with **2** residing at $\Delta H = +2.3$ kcal/mol relative to **1** + **I** (Figure 4). A plausible reaction pathway was calculated to involve initial dissociation of TMEDA, which is endothermic by +7.1 kcal/mol and provides the unsaturated intermediate **1′**. Nucleophilic attack of **I** at the linear two-coordinate zinc centre leads to the donor-acceptor complex **1″** with a long Zn1-Ga2 distance of 3.106 Å. Subsequent oxidative addition of the Zn–H bond at the Ga2 centre to give **2** was calculated to proceed via a 3-membered transition state, **TS1** at $\Delta H = +$ 17.0 kcal/mol.

C_6D_6 solutions of **1** or **1-*d*$_2$** were inert towards a ca. 1.5 bar of H_2 or D_2. No evidence was found for H/D exchange and although the expected hydrogenation product **I-H_2** (or **I–D_2**) was observed by ^{1}H NMR spectroscopy, its evolution was accompanied with formation of **I** and deposition of metallic zinc (see Supporting Information for further details). Isotopic labelling confirmed both hydride/deuteride ligands to derive from thermolysis of the heterobimetallic, rather than from reaction with H_2 or D_2.

Conclusions

[(BDI)Ga] (**I**) readily inserts into one or both Zn–H bond(s) of partially deaggregated zinc dihydride as hydrocarbon/TMEDA suspension by oxidative addition, providing the bimetallic and trimetallic hydridogallyl-zinc complexes **1** and **2**. Both insertion processes are reversible, and selectivity can be controlled by adjusting the stoichiometry of TMEDA. Decomposition to **I**, **I-H_2**, and metallic zinc is proposed to proceed via complex **2** and is thus inhibited by the presence of excess TMEDA. These results demonstrate the effect of labile ligands on controlling formal oxidative addition and reductive elimination in main-group compounds.[15,22] Understanding the potentially dynamic solution-state behaviour of reduced heterobimetallic complexes is of relevance to the application of such species in small-molecule activation and catalysis.

Experimental section

Full details of all experiments and characterisation data of the described compounds are given in the Supporting Information.

Synthesis and characterisation of [(BDI)Ga(H)-(H)Zn{tmeda}] (1)

A Schlenk flask was charged with $[ZnH_2]_n$ (14.5 mg, 0.215 mmol)[20a,21a] and [(BDI)Ga] (**I**) (100 mg 0.205 mmol).[24] TMEDA (117 mg, 1.0 mmol) and benzene (5 mL) were added and the reaction mixture was rapidly stirred, resulting in the formation of a bright yellow solution. The reaction mixture was stirred at room temperature for 1 h, then passed through a cannula filter. Compound **1** was obtained as a yellow powder upon removal of all volatiles and stripping of residual TMEDA with *n*-pentane. Yield 78 mg, 56%. Single crystals suitable for X-ray diffraction analysis were obtained from an *n*-hexane/toluene solution at −35 °C. Compound **1** is indefinitely stable in the solid state at −35 °C, and stable in benzene solution for at least a week in the presence of an excess (>5 equiv.) of TMEDA, but otherwise decomposes over the course of a day in hydrocarbon solvents. Here, the ^{1}H and ^{13}C NMR characterisation data is reported in pure C_6D_6, and those recorded in TMEDA-stabilised C_6D_6 solutions are detailed in the Supporting Information, as are experimental procedures for preparation of **1-*d*$_2$**.

^{1}H NMR (400 MHz, C_6D_6): δ 7.29–7.20 (m, 2H, *para*-dipp), 7.13–7.10 (m, 4H, *meta*-dipp), 6.36 (d, J=10.9 Hz, 1H, Ga-*H*), 4.88 (s, 1H, *H*C{(CNdipp)CH_3)}$_2$), 4.55 (d, J=11.7 Hz, 1H, Zn-*H*), 4.03 (hept, J=

6.8 Hz, 2H, $HC(CH_3)_2$)), 3.60 (hept, $J=6.8$ Hz, 2H, $HC(CH_3)_2$)), 2.31 (br, 1H, NCH_2-uncomplexed), 2.09 (br, 4H, NCH_3-uncomplexed), 1.77 (d, $J=6.8$ Hz, 6H, $HC(CH_3)_2$), 1.74 (s, 6H, $HC\{(CNdipp)CH_3)\}_2$), 1.73–1.57 (br, 16H, NCH_2+NCH_3), 1.38 (d, $J=6.7$ Hz, 6H, $HC(CH_3)_2$), 1.30 (d, $J=$ 6.9 Hz, 6H, $HC(CH_3)_2$), 1.21 (d, $J=6.9$ Hz, 6H, $HC(CH_3)_2$).*some integrals deviate from the expected values due to overlapping with decomposition products **I** and **2**.

$^{13}C\{^1H\}$ NMR (101 MHz, C_6D_6): δ 166.18 ($HC\{(CNdipp)CH_3)\}_2$), 145.72 (*ipso*-dipp), 145.31 (*ortho*-dipp), 143.75 (*ortho*-dipp), 125.38 (*meta*-dipp), 124.36 (*meta*-dipp), 123.94 (*para*-dipp), 93.86 ($HC\{(CNdipp)CH_3)\}_2$), 57.27 (br, NCH_2), 47.98 (br, NCH_3), 29.61 ($HC(CH_3)_2$), 27.68 ($HC(CH_3)_2$), 26.84 85 ($HC(CH_3)_2$), 25.24 ($HC(CH_3)_2$), 24.74 ($HC(CH_3)_2$), 24.61 ($HC(CH_3)_2$), 23.57 ($HC\{(CNdipp)CH_3)\}_2$).

Analysis calculated for $C_{35}H_{59}GaN_4Zn$: C, 62.65; H, 8.86; N, 8.35%. Found: C, 62.43; H, 8.62; N, 8.67%.

IR (KBr pellet): $\nu=1641$, 1581 cm^{-1} (Ga–H, Zn–H).

Synthesis and characterisation of [(BDI)GaH}$_2$Zn] (2)

In the glove box, a Schlenk flask was charged with $[ZnH_2]_n$ (12 mg, 0.205 mmol) and [(BDI)Ga] (**I**) (100 mg, 0.178 mmol). A 5 mL *n*-pentane solution of TMEDA (2.4 mg, 0.021 mmol) was added by pipette. The reaction mixture was stirred for 90 min., resulting in a cloudy bright-yellow solution, which was cycled onto a Schlenk line and cooled to −78 °C for 15 minutes to encourage precipitation of by-product **1** and supress disproportionation. Cannula filtration at this temperature provided a bright yellow solution from which volatiles were removed under vacuum to provide a yellow powder, identified as a 2:1 mixture of [{(BDI)GaH}$_2$Zn] (**2**) and **I** by ^1H NMR spectroscopy. Compound **2** was extracted from the crude product with minimal *n*-pentane, filtered, and stored at −35 °C for several days to obtain single crystals of **2** as yellow rods suitable for X-ray diffraction analysis. Yield 34 mg, 16%. Compound **2** is unstable in solution; isolated samples completely decomposed to an equimolar solution of **I** and [(BDI)GaH_2] (**I-H_2**) over the course of 10 h with concomitant deposition of metallic zinc. As a result, ^{13}C NMR data was obtained at 273 K.

^1H NMR (400 MHz, 298 K, C_6D_6): δ 7.15–7.02 (m, 5H, *meta*-dipp), 6.97 (dd, $J=7.5$, 1.6 Hz, 2H, *para*-dipp), 5.86 (br, 1H, Ga*H*), 4.68 (s, 1H, *H*C $\{(CNdipp)CH_3)\}_2$), 3.37 (2x overlapping hept, $J=6.9$ Hz, 4H, *H*C-$(CH_3)_2$)), 1.49 (s, 6H, $HC\{(CNdipp)CH_3)\}_2$), 1.26 (d, $J=6.7$ Hz, 7H, $HC(CH_3)_2$), 1.20 (d, $J=6.7$ Hz, 7H, $HC(CH_3)_2$), 1.10 (two overlapping doublets, $J=6.9$, 12H, $HC(CH_3)_2$). *Some integrals deviate from the expected values due to overlapping peaks assigned to decomposition products.

^1H NMR (400 MHz, toluene-d_8, 273 K): δ 7.10–7.00 (m, 4H, dipp),* 6.94 (m, dipp), 5.78 (s, 1H, Ga*H*), 4.63 (s, 1H, $HC\{(CNdipp)CH_3)\}_2$), 3.42-3.22 (2x overlapping hept, $J=6.9$, 6.8 Hz, 4H, $HC(CH_3)_2$)), 1.47 (s, 6H, $HC\{(CNdipp)CH_3)\}_2$), 1.22 (2x overlapped d, $J=6.8$, 6.8 Hz, 13H, $HC(CH_3)_2$),** 1.10 (d, $J=6.7$ Hz, 6H, $HC(CH_3)_2$), 1.05 (d, $J=$ 6.9 Hz, 6H, $HC(CH_3)_2$).* overlaps with solvent.**Inaccurate integral due to overlapped decomposition product.

$^{13}C\{^1H\}$ NMR (101 MHz, toluene-d_8, 273 K): δ 166.84 $HC\{(CNdipp)CH_3)\}_2$, 144.76 (1-dipp), 141.44 (2,6-Dipp), 126.34 (3,5-Dipp), 124.54 (3,5-Dipp), 123.86 (4-Dipp), 94.66 ($HC\{(CNdipp)CH_3)\}_2$), 29.26 ($HC(CH_3)_2$), 27.64 ($HC(CH_3)_2$), 27.22 ($HC(CH_3)_2$), 24.93 ($HC(CH_3)_2$), 24.82 ($HC(CH_3)_2$), 24.04 ($HC(CH_3)_2$), 22.87 ($HC\{(CNdipp)CH_3)\}_2$).

We were unable to obtain meaningful elemental analysis due to low thermal stability and high air/moisture sensitivity of this compound.

IR (KBr pellet): $\nu=1638$ cm^{-1} (Ga–H).

Deposition Number(s) 2170768 (**1**) and 2170769 (**2**) contain the supplementary crystallographic data for this paper. These data are provided free of charge by the joint Cambridge Crystallographic Data Centre and Fachinformationszentrum Karlsruhe Access Structures service.

Acknowledgements

We thank the Deutsche Forschungsgemeinschaft for financial support. We acknowledge Dr. G. Fink for assisting with NMR experiments, and Prof. Dr. U. Englert and Dr. T. P. Spaniol for advice regarding crystal structure refinement. L.M. is a senior member of the Institut Universitaire de France. The Alexander von Humboldt Foundation is acknowledged for financial support as well as CalMip for a generous grant of computing time. Open Access funding enabled and organized by Projekt DEAL.

Conflict of Interest

The authors declare no conflict of interest.

Data Availability Statement

The data that support the findings of this study are available in the supplementary material of this article.

Keywords: gallium · heterometallic complexes · hydrides · zinc

[1] a) M. M. D. Roy, A. A. Omana, A. S. S. Wilson, M. S. Hill, S. Aldridge, E. Rivard, *Chem. Rev.* **2021**, *121*, 12784–12965; b) W. L. Li, X. L. Ma, M. G. Walawalkar, Z. Yang, H. W. Roesky, *Coord. Chem. Rev.* **2017**, *350*, 14–29; c) G. I. Nikonov, *ACS Catal.* **2017**, *7*, 7257–7266; d) M. S. Hill, D. J. Liptrot, C. Weetman, *Chem. Soc. Rev.* **2016**, *45*, 972–988; e) T. J. Hadlington, M. Driess, C. Jones, *Chem. Soc. Rev.* **2018**, *47*, 4176–4197.
[2] a) S. E. Clapham, A. Hadzovic, R. H. Morris, *Coord. Chem. Rev.* **2004**, *248*, 2201–2237; b) D. Evans, J. A. Osborn, F. H. Jardine, G. Wilkinson, *Nature* **1965**, *208*, 1203–1204.
[3] a) I. Wender, H. W. Sternberg, M. Orchin, *J. Am. Chem. Soc.* **1953**, *75*, 3041–3042; b) F. Hebrard, P. Kalck, *Chem. Rev.* **2009**, *109*, 4272–4282.
[4] B. H. Davis, *Fuel Process. Technol.* **2001**, *71*, 157–166.
[5] a) P. Stoltze, J. K. Norskov, *Phys. Rev. Lett.* **1985**, *55*, 2502–2505; b) J. P. Guo, P. Chen, *Nat. Catal.* **2021**, *4*, 734–735.
[6] a) R. M. Charles, T. P. Brewster, *Coord. Chem. Rev.* **2021**, *433*, 213765; b) M. A. Stevens, A. L. Colebatch, *Chem. Soc. Rev.* **2022**, *51*, 1881-1898; c) R. C. Cammarota, C. C. Lu, *J. Am. Chem. Soc.* **2015**, *137*, 12486–12489; d) Y. P. Cai, S. J. Jiang, L. Q. Dong, X. Xu, *Dalton Trans.* **2022**, *51*, 3817–3827; e) N. Saito, J. Takaya, N. Iwasawa, *Angew. Chem. Int. Ed.* **2019**, *58*, 9998–10002; *Angew. Chem.* **2019**, *131*, 10103–10107; f) N. Hara, T. Saito, K. Semba, N. Kuriakose, H. Zheng, S. Sakaki, Y. Nakao, *J. Am. Chem. Soc.* **2018**, *140*, 7070–7073.
[7] a) T. N. Hooper, S. Lau, W. Y. Chen, R. K. Brown, M. Garçon, K. Luong, N. S. Barrow, A. S. Tatton, G. A. Sackman, C. Richardson, A. J. P. White, R. I. Cooper, A. J. Edwards, I. J. Casely, M. R. Crimmin, *Chem. Sci.* **2019**, *10*, 8083–8093; b) M. Garçon, C. Bakewell, G. A. Sackman, A. J. P. White, R. I. Cooper, A. J. Edwards, M. R. Crimmin, *Nature* **2019**, *574*, 390–393; c) S. Lau, A. J. P. White, I. J. Casely, M. R. Crimmin, *Organometallics* **2018**, *37*, 4521–4526; d) J. Turner, J. A. B. Abdalla, J. I. Bates, R. Tirfoin, M. J. Kelly, N. Phillips, S. Aldridge, *Chem. Sci.* **2013**, *4*, 4245–4250; e) J. A. B. Abdalla, I. M. Riddlestone, J. Turner, P. A. Kaufman, R. Tirfoin, N. Phillips, S. Aldridge, *Chem. Eur. J.* **2014**, *20*, 17624–17634; f) M. J. Butler, M. R.

Crimmin, *Chem. Commun.* **2017**, *53*, 1348–1365; g) A. Caise, J. A. B. Abdalla, R. Tirfoin, A. J. Edwards, S. Aldridge, *Chem. Eur. J.* **2017**, *23*, 16906–16913; h) O. Ekkert, A. J. P. White, M. R. Crimmin, *Angew. Chem. Int. Ed.* **2016**, *55*, 16031–16034; *Angew. Chem.* **2016**, *128*, 16265–16268; i) O. Ekkert, A. J. P. White, H. Toms, M. R. Crimmin, *Chem. Sci.* **2015**, *6*, 5617–5622; j) I. M. Riddlestone, J. A. B. Abdalla, S. Aldridge, in *Adv. Organomet. Chem., Vol. 63* (Ed.: P. J. Perez), **2015**, pp. 1–38; k) A. E. Nako, Q. W. Tan, A. J. P. White, M. R. Crimmin, *Organometallics* **2014**, *33*, 2685–2688; l) J. L. Vincent, S. Luo, B. L. Scott, R. Butcher, C. J. Unkefer, C. J. Burns, G. J. Kubas, A. Lledos, F. Maseras, J. Tomas, *Organometallics* **2003**, *22*, 5307–5323; m) M. Chen, S. Jiang, L. Maron, X. Xu, *Dalton Trans.* **2019**, *48*, 1931–1935; n) S. Jiang, Y. Cai, A. Carpentier, I. del Rosal, L. Maron, X. Xu, *Chem. Commun.* **2021**, *57*, 13696–13699.

[8] a) T. N. Hooper, M. Garçon, A. J. P. White, M. R. Crimmin, *Chem. Sci.* **2018**, *9*, 5435–5440; b) M. Garçon, N. W. Mun, A. J. P. White, M. R. Crimmin, *Angew. Chem. Int. Ed.* **2021**, *60*, 6145–6153; *Angew. Chem.* **2021**, *133*, 6210–6218; c) M. Garçon, A. J. P. White, M. R. Crimmin, *Chem. Commun.* **2018**, *54*, 12326–12328.

[9] a) R. K. Brown, T. N. Hooper, F. Rekhroukh, A. J. P. White, P. J. Costa, M. R. Crimmin, *Chem. Commun.* **2021**, *57*, 11673–11676; b) T. N. Hooper, R. K. Brown, F. Rekhroukh, M. Garcon, A. J. P. White, P. J. Costa, M. R. Crimmin, *Chem. Sci.* **2020**, *11*, 7850–7857.

[10] a) F. Rekhroukh, W. Y. Chen, R. K. Brown, A. J. P. White, M. R. Crimmin, *Chem. Sci.* **2020**, *11*, 7842–7849; b) C. Bakewell, B. J. Ward, A. J. P. White, M. R. Crimmin, *Chem. Sci.* **2018**, *9*, 2348–2356; c) W. Y. Chen, T. N. Hooper, J. Ng, A. J. P. White, M. R. Crimmin, *Angew. Chem. Int. Ed.* **2017**, *56*, 12687–12691; *Angew. Chem.* **2017**, *129*, 12861–12865.

[11] P. P. Power, *Nature* **2010**, *463*, 171–177.

[12] S. Brand, H. Elsen, J. Langer, S. Grams, S. Harder, *Angew. Chem. Int. Ed.* **2019**, *58*, 15496–15503; *Angew. Chem.* **2019**, *131*, 15642–15649.

[13] a) T. Chu, G. I. Nikonov, *Chem. Rev.* **2018**, *118*, 3608–3680; b) T. Chu, Y. Boyko, I. Korobkov, G. I. Nikonov, *Organometallics* **2015**, *34*, 5363–5365; c) T. Chu, I. Korobkov, G. I. Nikonov, *J. Am. Chem. Soc.* **2014**, *136*, 9195–9202; d) C. Ganesamoorthy, D. Blaser, C. Wolper, S. Schulz, *Organometallics* **2015**, *34*, 2991–2996; e) C. Ganesamoorthy, D. Blaser, C. Wolper, S. Schulz, *Chem. Commun.* **2014**, *50*, 12382–12384; f) C. Ganesamoorthy, D. Blaser, C. Wolper, S. Schulz, *Angew. Chem. Int. Ed.* **2014**, *53*, 11587–11591; *Angew. Chem.* **2014**, *126*, 11771–11775; g) A. Paparo, C. Jones, *Chem. Asian J.* **2019**, *14*, 486–490.

[14] a) R. L. Falconer, G. S. Nichol, I. V. Smolyar, S. L. Cockroft, M. J. Cowley, *Angew. Chem. Int. Ed.* **2021**, *60*, 2047–2052; *Angew. Chem.* **2021**, *133*, 2075–2080; b) A. Hofmann, T. Troster, T. Kupfer, H. Braunschweig, *Chem. Sci.* **2019**, *10*, 3421–3428; c) A. Hofmann, A. Lamprecht, J. O. C. Jimenez-Halla, T. Troster, R. D. Dewhurst, C. Lenczyk, H. Braunschweig, *Chem. Eur. J.* **2018**, *24*, 11795–11802; d) A. Kempter, C. Gemel, R. A. Fischer, *Inorg. Chem.* **2008**, *47*, 7279–7285; e) R. Rodriguez, Y. Contie, R. Nougue, A. Baceiredo, N. Saffon-Merceron, J. M. Sotiropoulos, T. Kato, *Angew. Chem. Int. Ed.* **2016**, *55*, 14353–14356; *Angew. Chem.* **2016**, *128*, 14567–14570; f) J. D. Erickson, R. D. Riparetti, J. C. Fettinger, P. P. Power, *Organometallics* **2016**, *35*, 2124–2128; g) J. D. Erickson, J. C. Fettinger, P. P. Power, *Inorg. Chem.* **2015**, *54*, 1940–1948.

[15] L. J. Morris, A. Carpentier, L. Maron, J. Okuda, *Chem. Commun.* **2021**, *57*, 9454–9457.

[16] C. Ganesamoorthy, J. Schoening, C. Wolper, L. J. Song, P. R. Schreiner, S. Schulz, *Nat. Chem.* **2020**, *12*, 608–614.

[17] a) F. M. Miloserdov, A. F. Pecharman, L. Sotorrios, N. A. Rajabi, J. P. Lowe, S. A. Macgregor, M. F. Mahon, M. K. Whittlesey, *Inorg. Chem.* **2021**, *60*, 16256–16265; b) F. M. Miloserdov, N. Rajabi, J. P. Lowe, M. F. Mahon, S. A. Macgregor, M. K. Whittlesey, *J. Am. Chem. Soc.* **2020**, *142*, 6340–6349; c) M. Espinal-Viguri, V. Varela-Izquierdo, F. M. Miloserdov, I. M. Riddlestone, M. F. Mahon, M. K. Whittlesey, *Dalton Trans.* **2019**, *48*, 4176–4189; d) I. M. Riddlestone, N. A. Rajabi, J. P. Lowe, M. F. Mahon, S. A. Macgregor, M. K. Whittlesey, *J. Am. Chem. Soc.* **2016**, *138*, 11081–11084; e) D. J. Cole-Hamilton, G. Wilkinson, *J. Chem. Soc. Dalton Trans.* **1977**, 797–804; f) F. N. Tebbe, *J. Am. Chem. Soc.* **1973**, *95*, 5412–5414; g) M. Ohashi, K. Matsubara, T. Iizuka, H. Suzuki, *Angew. Chem. Int. Ed.* **2003**, *42*, 937–940; *Angew. Chem.* **2003**, *115*, 967–970; h) B. Fischer, H. Kleijn, J. Boersma, G. van Koten, A. L. Spek, *Organometallics* **1989**, *8*, 920–925; i) P. H. M. Budzelaar, K. H. Denhaan, J. Boersma, G. J. M. van der Kerk, A. L. Spek, *Organometallics* **1984**, *3*, 156–159; j) M. D. Fryzuk, D. H. McConville, S. J. Rettig, *Organometallics* **1993**, *12*, 2152–2161; k) P. D. Bolton, E. Clot, A. R. Cowley, P. Mountford, *J. Am. Chem. Soc.* **2006**, *128*, 15005–15018; l) M. van Meurs, G. J. P. Britovsek, V. C. Gibson, S. A. Cohen, *J. Am. Chem. Soc.* **2005**, *127*, 9913–9923; m) G. J. P. Britovsek, S. A. Cohen, V. C. Gibson, M. van Meurs, *J. Am. Chem. Soc.* **2004**, *126*, 10701–10712.

[18] a) A. Kempter, C. Gemel, T. Cadenbach, R. A. Fischer, *Inorg. Chem.* **2007**, *46*, 9481–9487; b) O. Bonello, C. Jones, A. Stasch, W. D. Woodul, *Organometallics* **2010**, *29*, 4914–4922; c) C. Jones, R. P. Rose, A. Stasch, *Dalton Trans.* **2007**, 2997–2999.

[19] M. Plois, R. Wolf, W. Hujo, S. Grimme, *Eur. J. Inorg. Chem.* **2013**, 3039–3048.

[20] a) G. D. Barbaras, C. Dillard, A. E. Finholt, T. Wartik, K. E. Wilzbach, H. I. Schlesinger, *J. Am. Chem. Soc.* **1951**, *73*, 4585–4590; b) J. J. Watkins, E. C. Ashby, *Inorg. Chem.* **1974**, *13*, 2350–2354.

[21] a) F. Ritter, L. J. Morris, K. N. McCabe, T. P. Spaniol, L. Maron, J. Okuda, *Inorg. Chem.* **2021**, *60*, 15583–15592; b) F. Ritter, T. P. Spaniol, I. Douair, L. Maron, J. Okuda, *Angew. Chem. Int. Ed.* **2020**, *59*, 23335–23342; *Angew. Chem.* **2020**, *132*, 23535–23543; c) A. Rit, T. P. Spaniol, L. Maron, J. Okuda, *Angew. Chem. Int. Ed.* **2013**, *52*, 4664–4667; *Angew. Chem.* **2013**, *125*, 4762–4765; d) N. A. Bell, A. L. Kassyk, *J. Organomet. Chem.* **1988**, *345*, 245–251; e) X. M. Wang, X. Xu, *RSC Adv.* **2021**, *11*, 1128–1133; f) F. Ritter, K. N. McCabe, L. Maron, T. P. Spaniol, J. Okuda, *Polyhedron* **2021**, *204*, 115264; g) P. A. Lummis, M. R. Momeni, M. W. Lui, R. McDonald, M. J. Ferguson, M. Miskolzie, A. Brown, E. Rivard, *Angew. Chem. Int. Ed.* **2014**, *53*, 9347–9351; *Angew. Chem.* **2014**, *126*, 9501–9505.

[22] a) L. J. Morris, P. Ghana, T. Rajeshkumar, A. Carpentier, L. Maron, J. Okuda, *Angew. Chem. Int. Ed.* **2022**, e202114629; *Angew. Chem.* **2022**, e202114629; b) A. Caise, L. P. Griffin, A. Heilmann, C. McManus, J. Campos, S. Aldridge, *Angew. Chem. Int. Ed.* **2021**, *60*, 15606–15612; c) A. Caise, A. E. Crumpton, P. Vasko, J. Hicks, C. McManus, N. H. Rees, S. Aldridge, *Angew. Chem. Int. Ed.* **2022**, e202114926.

[23] M. Asay, C. Jones, M. Driess, *Chem. Rev.* **2011**, *111*, 354–396.

[24] a) N. J. Hardman, B. E. Eichler, P. P. Power, *Chem. Commun.* **2000**, 1991–1992; b) O. Kysliak, H. Gorls, R. Kretschmer, *Dalton Trans.* **2020**, *49*, 6377–6383.

[25] S. Singh, H. J. Ahn, A. Stasch, V. Jancik, H. W. Roesky, A. Pal, M. Biadene, R. Herbst-Irmer, M. Noltemeyer, H. G. Schmidt, *Inorg. Chem.* **2006**, *45*, 1853–1860.

[26] A. Seifert, D. Scheid, G. Linti, T. Zessin, *Chem. Eur. J.* **2009**, *15*, 12114–12120.

[27] a) C. A. Caputo, J. Koivistoinen, J. Moilanen, J. N. Boynton, H. M. Tuononen, P. P. Power, *J. Am. Chem. Soc.* **2013**, *135*, 1952–1960; b) Z. L. Zhu, X. P. Wang, Y. Peng, H. Lei, J. C. Fettinger, E. Rivard, P. P. Power, *Angew. Chem. Int. Ed.* **2009**, *48*, 2031–2034; *Angew. Chem.* **2009**, *121*, 2065–2068.

[28] L. J. Morris, T. Rajeshkumar, A. Okumura, L. Maron, J. Okuda, *Angew. Chem. Int. Ed.* **2022**, e202208855; *Angew. Chem.* **2022**, e202208855.

[29] a) M. Molon, C. Gemel, R. W. Seidel, P. Jerabek, G. Frenking, R. A. Fischer, *Inorg. Chem.* **2013**, *52*, 7152–7160; b) M. Molon, K. Dilchert, C. Gemel, R. W. Seidel, J. Schaumann, R. A. Fischer, *Inorg. Chem.* **2013**, *52*, 14275–14283; c) P. Heiss, J. Hornung, X. Y. Zhou, C. Jandl, A. Pothig, C. Gemel, R. A. Fischer, *Inorg. Chem.* **2020**, *59*, 514–522.

[30] a) K. Freitag, H. Banh, C. Gemel, P. Jerabek, R. W. Seidel, G. Frenking, R. A. Fischer, *Inorg. Chem.* **2015**, *54*, 352–358; b) I. L. Fedushkin, A. N. Lukoyanov, A. N. Tishkina, M. O. Maslov, S. Y. Ketkov, M. Hummert, *Organometallics* **2011**, *30*, 3628–3636; c) I. L. Fedushkin, A. N. Lukoyanov, S. Y. Ketkov, M. Hummert, H. Schumann, *Chem. Eur. J.* **2007**, *13*, 7050–7056.

[31] a) J. D. Queen, S. Irvankoski, J. C. Fettinger, H. M. Tuononen, P. P. Power, *J. Am. Chem. Soc.* **2021**, *143*, 6351–6356; b) K. L. Mears, C. R. Stennett, E. K. Taskinen, C. E. Knapp, C. J. Carmalt, H. M. Tuononen, P. P. Power, *J. Am. Chem. Soc.* **2020**, *142*, 19874–19878; c) P. P. Power, *Organometallics* **2020**, *39*, 4127–4138; d) D. J. Liptrot, P. P. Power, *Nat. Rev. Chem.* **2017**, *1*, 0004; e) J. D. Guo, D. J. Liptrot, S. Nagase, P. P. Power, *Chem. Sci.* **2015**, *6*, 6235–6244; f) C. R. Stennett, M. Bursch, J. C. Fettinger, S. Grimme, P. P. Power, *J. Am. Chem. Soc.* **2021**, *143*, 21478–21483.

[32] J. Hicks, E. J. Underhill, C. E. Kefalidis, L. Maron, C. Jones, *Angew. Chem. Int. Ed.* **2015**, *54*, 10000–10004; *Angew. Chem.* **2015**, *127*, 10138–10142.

[33] A. L. Allred, *J. Inorg. Nucl. Chem.* **1961**, *17*, 215–221.

[34] a) C. P. White, J. Braddock-Wilking, J. Y. Corey, H. Xu, E. Redekop, S. Sedinkin, N. P. Rath, *Organometallics* **2007**, *26*, 1996–2004; b) M. Usher, A. V. Protchenko, A. Rit, J. Campos, E. L. Kolychev, R. Tirfoin, S. Aldridge, *Chem. Eur. J.* **2016**, *22*, 11685–11698; c) M. Oishi, M. Kino, M. Saso, M. Oshima, H. Suzuki, *Organometallics* **2012**, *31*, 4658–4661; d) N. Nakata, S. Fukazawa, N. Kato, A. Ishii, *Organometallics* **2011**, *30*, 4490–4493; e) M. L. McCrea-Hendrick, S. Wang, K. L. Gullett, J. C. Fettinger, P. P. Power, *Organometallics* **2017**, *36*, 3799–3805; f) K. E. Litz, K. Henderson,

R. W. Gourley, M. M. B. Holl, *Organometallics* **1995**, *14*, 5008–5010; g) T. Fukuda, H. Hashimoto, H. Tobita, *J. Organomet. Chem.* **2017**, *848*, 89–94; h) T. P. Dhungana, H. Hashimoto, H. Tobita, *Dalton Trans.* **2017**, *46*, 8167–8179; i) S. M. I. Al-Rafia, M. R. Momeni, M. J. Ferguson, R. McDonald, A. Brown, E. Rivard, *Organometallics* **2013**, *32*, 6658–6665.

[35] B. Rösch, T. X. Gentner, J. Eyselein, J. Langer, H. Elsen, S. Harder, *Nature* **2021**, *592*, 717–721.

[36] For this experiment, compound **2** was generated in situ by reaction of **I** with two equiv. of $[ZnH_2]_n$ in the presence of 7 mol% TMEDA, then immediately filtered to remove excess $[ZnH_2]_n$ before addition of 7 equiv. of TMEDA.

Manuscript received: May 13, 2022
Accepted manuscript online: July 12, 2022
Version of record online: August 22, 2022